ORGANOMETALLICS

Formation of .beta.-CH agostic alkenylzirconocene complexes

Isabella Hyla-Kryspin, Rolf Gleiter, Carl Krueger, Roland Zwettler, and Gerhard Erker

Organometallics, **1990**, 9 (2), 517-523• DOI: 10.1021/om00116a033 • Publication Date (Web): 01 May 2002

Organometallics **1990,** *9,* 517-523 517

Formation of β-CH Agostic Alkenylzirconocene Complexes

Isabella Hyla-Kryspin,[†] Rolf Gleiter,*[,†] Carl Krüger,*[,‡] Roland Zwettler,[‡,§] and Gerhard Erker*[,§]

Institut für Organische Chemie der Universität Heidelberg, Im Neuenheimer Feld, D-6900 Heidelberg, FRG,
Max-Planck-Institut für Kohlenforschung, Kaiser-Wilhelm-Platz 1,
D-4330 Mülheim a. d. Ruhr, FRG, and Institut für Organische Chemie der
Universität Würzburg, Am Hubland, D-8700 Würzburg, FRG

Received July 31, 1989

Reaction of phenyl(trimethylsilyl)acetylene with hydridozirconocene chloride yields the β-CH agostic alkenylzirconocene chloride $Cp_2ZrCl[-C(SiMe_3)=CHPh]$ (**2a**). Halogen exchange with lithium bromide or iodide produces the analogous alkenylzirconocene bromide **2b** and iodide **2c**, respectively. In contrast, hydrozirconation of (trimethylsilyl)acetylene gives $Cp_2ZrCl(-CH=CHSiMe_3)$ (**4**), exhibiting the bulky $SiMe_3$ substituent at the β-position of the σ-alkenyl ligand, which lacks the β-agostic metal–C–H interaction that is characteristic of **2**. The molecular structures of **2b** and **4** were determined by X-ray diffraction. Complex **2b** crystallizes in space group $P2_1/n$ with cell constants a = 9.746 (1) Å, b = 17.968 (3) Å, c = 11.887 (1) Å, β = 90.46 (1)°, Z = 4, R = 0.051, and R_w = 0.049. The alkenylmetallocene **4** crystallizes in space group $P2_1/c$ with cell parameters a = 10.866 (1) Å, b = 12.457 (1) Å, c = 13.373 (2) Å, β = 110.80 (1)°, Z = 4, R = 0.046, and R_w = 0.048. Model calculations have confirmed that steric in addition to electronic factors are mainly responsible for the formation of the β-CH agostic interaction in the alkenylzirconocene complexes **2**.

Introduction

Organometallic compounds exhibiting "agostic" M–H–C interactions are known of most d-group elements.[1] Intramolecular coordination of a C–H bond requires a suitable metal acceptor orbital and favorable steric and electronic features of the carbon–hydrogen bond that is to be "activated". The strong electrophilicity of the coordinatively unsaturated metal center seems to govern the M–H–C three-center–two-electron interaction in typical early-transition-metal agostic complexes such as $(dmpe)Cl_3TiCH_3$ and $(dmpe)Cl_3TiCH_2CH_3$.[2] Use of the much less electrophilic 16-electron center in compounds such as Cp_2MXY means that the formation of an agostic M–H–C bond is only favorable in borderline cases and that small changes in the spatial orientation and/or the electron density in the ligand C–H bond may be decisive.

We have recently shown that the C=C—H carbon–hydrogen bond in complexes **1a** and **1b** coordinates to the 16-electron bis(cyclopentadienyl)zirconium center at the β-alkenyl sp^2 carbon atom.[3] The alkyne hydrozirconation reaction provides for an easy synthesis of $Cp_2ZrCl[-CR^1=CHR^2]$ complexes.[4] Such systems may, therefore, be suitable substrates for studying the important stereoelectronic factors at the σ-hydrocarbyl ligand leading to β-CH agostic bond formation. Using the σ-electron-donating, bulky $SiMe_3$ substituent (σ_I = −0.11) has enabled us to estimate the relative importance of steric and electronic factors responsible for the formation of a β C–H–Zr alkenyl interaction.

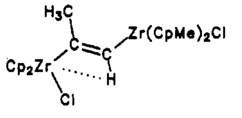

1a

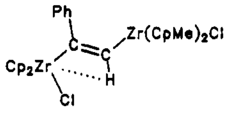

1b

Results

Experimental Studies. The Zr–H–C agostic zirconocene complexes **1a,b** are distinguished from ordinary nonagostic alkenylmetallocenes by characteristic spectroscopic features. The $[Zr]-C^\alpha=C^\beta-H$ unit shows a ^1H NMR signal at rather low field (δ 8.33 (**1a**), 8.11 (**1b**)). The ^{13}C NMR absorption of C^α is at δ 215.4 (**1a**) or 216.2 (**1b**), whereas the C^β signal is located upfield in the normal olefinic absorption range (δ 124.1 (**1a**), 135.9 (**1b**)). The very low $^1J(C^\beta-H)$ coupling constant (112 Hz (**1a**), 104 Hz (**1b**)) is a strong indication for the presence of the agostic metal–H–C moiety.

Scheme I

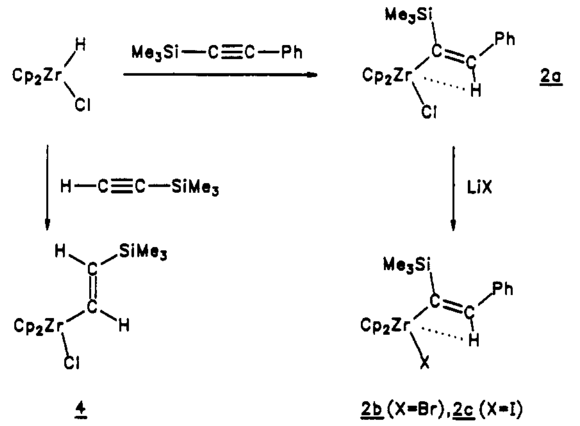

Hydrozirconation of phenyl(trimethylsilyl)acetylene cleanly yields the Me_3Si-substituted alkenylzirconocene

---

[†] Universität Heidelberg (calculations).

[‡] Max-Planck-Institut Mülheim (structures).

[§] Universität Würzburg (experimental work).

(1) For a recent comprehensive review see: Brookhart, M.; Green, M. L. H.; Wong, L.-L. *Prog. Inorg. Chem.* **1988,** *36,* 1.

(2) Dawoodi, Z.; Green, M. L. H.; Mtetwa, V. S. B.; Prout, K. *J. Chem. Soc., Chem. Commun.* **1982,** 802, 1410. Dawoodi, Z.; Green, M. L. H.; Mtetwa, V. S. B.; Prout, K.; Schultz, A. J.; Williams, J. M.; Koetzle, T. F. *J. Chem. Soc., Dalton Trans.* **1986,** 1629.

(3) Erker, G.; Frömberg, W.; Angermund, K.; Schlund, R.; Krüger, C. *J. Chem. Soc., Chem. Commun.* **1986,** 372.

(4) Schwartz, J.; Labinger, J. A. *Angew. Chem.* **1976,** *88,* 402.

(5) Preliminary communication: Erker, G.; Zwettler, R.; Krüger, C.; Schlund, R.; Hyla-Kryspin, I.; Gleiter, R. *J. Organomet. Chem.* **1988,** *346,* C15.

(6) Erker, G.; Kropp, K.; Atwood, J. L.; Hunter, W. E. *Organometallics* **1983,** *2,* 1555.

(7) Czisch, P.; Erker, G.; Korth, H.-G.; Sustman, R. *Organometallics* **1984,** *3,* 945.

(8) Thiele, K. H. Personal communication.

0276-7333/90/2309-0517$02.50/0 © 1990 American Chemical Society

Table I. Selected ^{13}C/^{1}H NMR Data for the Alkenylzirconocene Complexes Cp$_2$ZrX[–CR^1=CHR^2]^{a,b}

compd	X	R^1	R^2	–*C*R^1=	=*C*HR^2	ref
1a	Cl	CH$_3$	[Zr]	215.4	124.1 (112)/ 8.33	3
1b	Cl	Ph	[Zr]	216.2	135.9 (104)/ 8.11	3
2a	Cl	SiMe$_3$	Ph	206.8^c	113.3 (123)^c/ 8.59	*f*
2b	Br	SiMe$_3$	Ph	204.5^d	109.4 (120)^d/ 8.41	*f*
2c	I	SiMe$_3$	Ph	198.7^d	104.1 (111)^d/ 7.85	*f*
3a^c	Cl	H	Ph	177.7 (122)/ 7.76	140.5 (153)/ 6.70	6
3b	CH$_2$Ph	H	Ph	177.0 (117)/ 7.80	141.0 (150)/ 6.85	7
3c^c	Cl	CH$_3$	CH$_3$	190.4	115.2 (146)/ 5.70	5
3d^e	CH=CH$_2$	H	H	189.9 (131)/ 6.32	124.5 (155)/ 5.20	8
3e^e	CH=CHCH$_3$	H	CH$_3$	191.5 (115)/ 5.83	130.4 (149)/ 5.21	9
4	Cl	H	SiMe$_3$	202.7 (128)/ 8.03	143.3 (136)/ 6.63	*f*

^{a} Data given in the following order: ^{13}C chemical shift in ppm ($^1J_{CH}$ coupling constant in Hz)/^{1}H chemical shift in ppm. ^{b} In benzene-d_6 unless otherwise noted. ^{c} CDCl$_3$. ^{d} CD$_2$Cl$_2$. ^{e} Bis(η-pentamethylcyclopentadienyl)zirconium complex. ^{f} This work.

complex **2a**. Complex **2a** reacts with lithium bromide and iodide to give the halide-exchange products **2b** and **2c**, respectively. Complexes Cp$_2$Zr(X)[–C(SiMe$_3$)=CHPh] (**2a** (X = Cl), **2b** (X = Br), **2c** (X = I)) all show very characteristic ^{1}H and ^{13}C NMR features, being very similar to those of **1a** and **1b**. The ^{1}H NMR absorption around δ 8, the C$^{\alpha}$ ^{13}C NMR signals at ca. 200 ppm, and the typical C$^{\beta}$–H absorption (δ ~110, ^1J(CH) ≈ 120 Hz) indicate the formation of complexes containing a β-CH agostic alkenylzirconocene moiety, $[\overline{\mathrm{Zr}]\text{–C(SiMe}_3)\text{=CH}}\mathrm{Ph}$ (see Table I).

Hydrozirconation of monosubstituted alkynes HC≡CR gives a different type of alkenylzirconocene complex. The nonagostic alkenylmetallocene compounds **3** are readily distinguished from their agostic counterparts **2** by their NMR spectra. Complexes **3** characteristically exhibit a much smaller difference of the ^{13}C NMR shifts of the C$^{\alpha}$ and C$^{\beta}$ carbon atoms. The ^1J(C$^{\beta}$–H) coupling constant is in the typical olefinic range. Only the ^1J(C$^{\alpha}$–H) coupling constant is somewhat reduced. The C$^{\beta}$–H ^{1}H NMR absorption of **3** is shifted to high field as compared to that of complexes **2**. However, the C$^{\alpha}$–H signals are found in the δ 8 range. It has been argued that these values might indicate (although not conclusively prove) the presence of a weak α-CH agostic M–H–C interaction in these complexes[9] (for representative examples see Chart I and Table I).

Hydrozirconation of (trimethylsilyl)acetylene yields the alkenylmetallocene complex **4**. According to its spectroscopic data, this product clearly does not belong to the agostic type A alkenylzirconocene complexes (**1**, **2**) but rather to the type B complexes (**3**). However, even among these, complex **4** appears to occupy a quite extreme position, showing very low field C$^{\alpha}$–H NMR absorptions (^{1}H, δ 8.03; ^{13}C, δ 202.7) and a somewhat reduced ^1J(C$^{\beta}$–H) coupling constant of 136 Hz.

Chart I

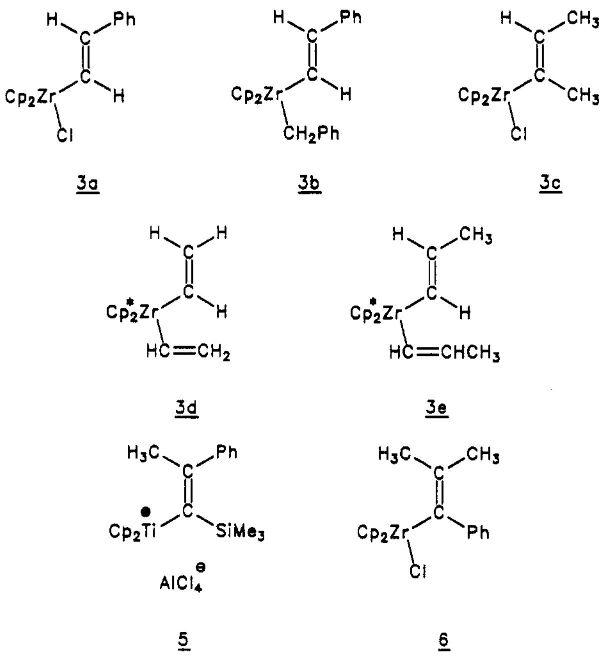

3a 3b 3c 3d 3e 5 6

X-ray Crystal Structure Analyses. The type A alkenylzirconocene complexes **2a**[5] and **2b** were characterized by X-ray diffraction. Complex **2a** exhibits a pseudotetrahedral bent metallocene unit. The trisubstituted σ-alkenyl ligand, comprising the carbon atoms C1, C2, and C3 (=ipso C of the phenyl substituent at C2) and Si, are oriented in the central major metallocene plane bisecting the Cp–Zr–Cp angle. The Me$_3$Si group is positioned at the alkenyl α-C atom, whereas the phenyl substituent is bonded to C$^{\beta}$. These two alkenyl substituents are orientated *Z* to each other. The C1–C2 distance is 1.339 (3) Å, not deviating very much from a typical averaged C=C bond distance of ordinary organic trisubstituted olefins (d(C=C) = 1.326 Å).[10] The Zr–C1 distance is 2.258 (2) Å, which is as expected for a zirconium to carbon σ-bond.[11] The Si–C1 distance is 1.867 (2) Å. The angles around the planar coordinated atom C1 are as follows: C2–C1–Si = 130.9 (2)°, Zr–C1–Si = 139.3 (1)°, Zr–C1–C2 = 89.9 (2)°. The notable deviations from ordinary C(sp^2) bond angles are caused by the pronounced agostic Zr–H2–C2 interaction. The Zr–C2 distance is short (2.623 (2) Å), as is the Zr–H2 separation of 2.29 (2) Å. The agostic C–H bond coordinates to zirconium in the major plane in a central position. The hydrogen atom H2 is thus placed in an intermediate position between the Zr–C1 and Zr–Cl vectors, making use of the only available acceptor orbital at the transition-metal center.[12] The zirconium–chlorine bond is rather long at 2.550 (1) Å, increased by about 0.1 Å as compared to typical Zr–Cl linkages in 16-electron

---

[9] McDade, C.; Bercaw, J. E. *J. Organomet. Chem.* **1985**, *279*, 281.

[10] Allen, F. H.; Kennard, O.; Watson, D. G.; Brammer, L.; Orpen, A. G.; Taylor, R. *J. Chem. Soc., Perkin Trans. 2* **1987**, S1.

[11] Cardin, D. J.; Lappert, M. F.; Raston, C. L. *Chemistry of Organo-Zirconium and -Hafnium Compounds*; Wiley: New York, 1986; and references cited therein.

[12] Lauher, J. W.; Hoffmann, R. *J. Am. Chem. Soc.* **1976**, *98*, 1729. Hofmann, P.; Stauffert, P.; Shore, N. *Chem. Ber.* **1982**, *115*, 2153.

Table II. Comparison of Selected Structural Parameters of Alkenylzirconocene Complexes $Cp_2ZrX[-CR^1{=}CR^2R^3]$[a]

compd	Zr–X	Zr–C1	C1–C2	X–Zr–C1	Zr–C1–C2	Zr–C1–R^1	ref
1a	2.577 (1)	2.209 (4)	1.328 (5)	116.9 (1)	90.4 (2)	140.6 (3)	3
2a	2.550 (1)	2.258 (2)	1.339 (3)	114.9 (1)	89.9 (2)	139.3 (1)	5
2b	2.721 (1)	2.265 (6)	1.322 (8)	115.8 (1)	88.7 (4)	139.4 (3)	*b*
4	2.441 (1)	2.267 (6)	1.217 (9)	96.6 (2)	144.2 (5)		*b*
5[c]		2.13	1.31		144.9	88.9	14
6	2.479 (1)	2.296 (3)	1.329 (5)	108.8 (1)	137.4 (3)	100.3 (3)	15

[a] Structural formulas of the complexes are given in the text. Atom-numbering schemes analogous to those in Figures 1 and 2 are used for all complexes throughout this table. Bond lengths are given in Å and bond angles in degrees with esd's in parentheses. [b] This work. [c] Cationic titanocene complex.

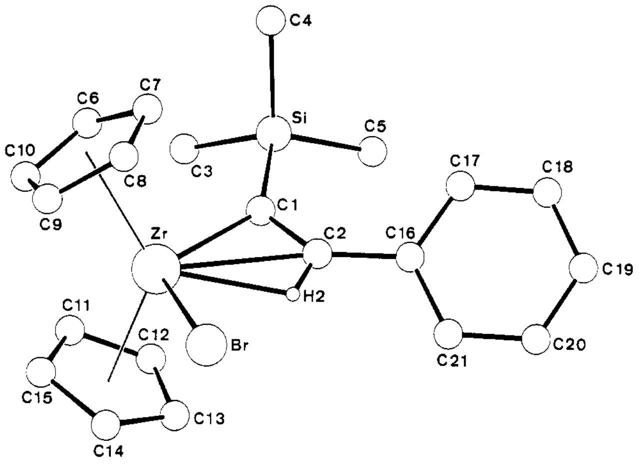

Figure 1. View of the molecular structure of the β-CH agostic alkenylzirconocene bromide **2b**.

Cp_2ZrXY complexes exhibiting purely tetracoordinated zirconium (e.g. $d(Zr–Cl)$ = 2.441 (10) Å in $(CH_2)_3(C_5H_4)_2ZrCl_2$, 2.447 (1) Å in $(C_5H_4SiMe_3)_2ZrCl[CH(SiMe_3)_2]$, and 2.452 (2) Å in $(C_5H_4CMe_3)_2ZrCl[CH(SiMe_3)_2]$).[11,13] The large Cl–Zr–C1 angle of 114.9 (1)° is typical for a pentacoordinated Cp_2Zr complex.[11]

The molecular structure of the alkenylzirconocene bromide **2b** is very similar (see Figure 1). The Br–Zr–C1 angle (115.8 (1)°) is only marginally increased. The pertinent bonding parameters around the α-alkenyl carbon atom C1 are $d(Zr–C1)$ = 2.265 (6) Å, $d(C1–C2)$ = 1.322 (8) Å, and Zr–C1–C2 = 88.7 (4)°. The Zr–C1–Si angle is 139.4 (3)°. The agostic hydrogen H2 is slightly closer to Zr ($d(Zr–H2)$ = 2.19 (5) Å) in the bromide-containing complex.

The molecular structure of the (trimethylsilyl)acetylene hydrozirconation product **4** differs quite considerably from those of **2a** and **2b**. The σ-alkenyl ligand bears the bulky trimethylsilyl substituent in the β-position, trans oriented to the Cp_2ZrCl moiety. The bonding parameters at the bent metallocene are as usually observed.[11,12] The Zr–C1 bond length is 2.267 (6) Å. The Zr–Cl distance is 2.441 (1) Å, i.e. much shorter than the metal–halogen distance in the β-agostic complex **2a**. The Cl–Zr–C1 angle of **4** is 96.6 (2)°, which is quite usual for a pseudotetrahedral zirconocene chloride with a 16-electron configuration of the central metal atom. These structural data do not indicate any significant α-CH agostic interaction in **4**, as has been

Table III. Positional Parameters of 2b

atom	*x*	*y*	*z*
Zr	0.0089 (1)	0.2169 (1)	0.3166 (1)
Br	−0.2227 (1)	0.2242 (1)	0.1878 (1)
Si	0.3349 (2)	0.0941 (1)	0.3044 (1)
C1	0.1760 (6)	0.1407 (3)	0.2525 (5)
C2	0.1124 (6)	0.1391 (4)	0.1539 (5)
C3	0.4269 (7)	0.1580 (5)	0.4031 (6)
C4	0.2932 (8)	0.0079 (4)	0.3813 (7)
C5	0.4626 (7)	0.0737 (4)	0.1914 (6)
C6	0.0496 (7)	0.1465 (4)	0.4988 (6)
C7	−0.0293 (8)	0.0991 (4)	0.4332 (6)
C8	−0.1569 (7)	0.1321 (4)	0.4167 (6)
C9	−0.1539 (8)	0.2004 (4)	0.4744 (6)
C10	−0.0271 (8)	0.2077 (4)	0.5253 (5)
C11	0.160 (1)	0.3192 (4)	0.3854 (6)
C12	0.2036 (7)	0.3055 (4)	0.2775 (7)
C13	0.1006 (7)	0.3249 (3)	0.2033 (5)
C14	−0.0080 (7)	0.3538 (4)	0.2656 (7)
C15	0.028 (1)	0.3502 (4)	0.3781 (7)
C16	0.1282 (6)	0.0985 (3)	0.0467 (5)
C17	0.1806 (6)	0.0270 (4)	0.0417 (5)
C18	0.1950 (7)	−0.0086 (4)	−0.0611 (7)
C19	0.1580 (8)	0.0255 (5)	−0.1577 (6)
C20	0.1051 (8)	0.0957 (5)	−0.1558 (6)
C21	0.0883 (7)	0.1324 (4)	−0.0534 (5)
H2	0.052 (6)	0.174 (3)	0.148 (5)

Table IV. Positional Parameters of 4

atom	*x*	*y*	*z*
Zr	0.2164 (1)	0.2209 (1)	0.1591 (1)
Cl	0.0680 (2)	0.1656 (1)	−0.0177 (1)
Si	0.6562 (1)	0.2274 (1)	0.1010 (1)
C1	0.4049 (5)	0.2098 (4)	0.1234 (5)
C2	0.5068 (6)	0.2561 (5)	0.1320 (6)
C3	0.7912 (6)	0.2016 (5)	0.2297 (6)
C4	0.6364 (7)	0.1121 (6)	0.0126 (6)
C5	0.6933 (6)	0.3474 (5)	0.0346 (5)
C6	0.3010 (6)	0.1376 (4)	0.3402 (4)
C7	0.3464 (6)	0.0717 (5)	0.2762 (5)
C8	0.2361 (7)	0.0236 (4)	0.2002 (5)
C9	0.1268 (5)	0.0579 (4)	0.2204 (4)
C10	0.1657 (5)	0.1284 (4)	0.3054 (4)
C11	0.2105 (8)	0.3820 (4)	0.2688 (5)
C12	0.3026 (5)	0.4042 (4)	0.2210 (6)
C13	0.2355 (9)	0.4149 (4)	0.1146 (6)
C14	0.1043 (8)	0.3976 (5)	0.0957 (7)
C15	0.0889 (7)	0.3743 (5)	0.1914 (8)

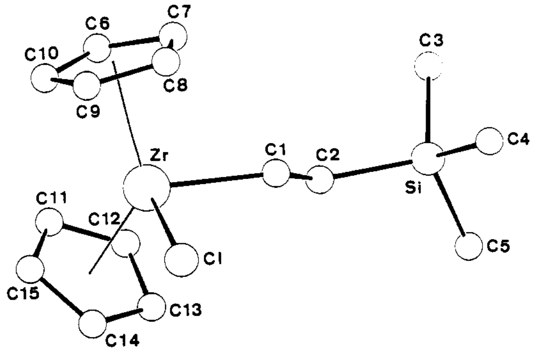

Figure 2. Molecular structure of $Cp_2ZrCl(-CH{=}CHSiMe_3)$ (**4**).

---

[13] Saldarriaga-Molina, C. H.; Clearfield, A.; Bernal, I. *Inorg. Chem.* **1974**, *13*, 2880. Lappert, M. F.; Riley, P. I.; Yarrow, P. I. W.; Atwood, J. L.; Hunter, W. E.; Zaworotko, M. J. *J. Chem. Soc., Dalton Trans.* **1981**, 814.

[14] (a) Eisch, J. J.; Piotrowski, A. M.; Brownstein, S. K.; Gabe, E. J.; Lee, F. L. *J. Am. Chem. Soc.* **1985**, *107*, 7219. (b) Koga, N.; Morokuma, K. *Ibid.* **1988**, *110*, 108.

[15] Cardin, C. J.; Cardin, J.; Morton-Blake, D. A.; Parge, H. E.; Roy, A. *J. Chem. Soc., Dalton Trans.* **1987**, 1641.

Table V. Calculated Values for α and β as Well as the Energy Differences for 1a, 1c, 2a, 3c, 3f, and 4 for Type A and Type B Conformations[a]

			A-type struct		B-type struct		
compd	R_1	R_2	α, deg	β, deg	α, deg	β, deg	E(A-B), kcal/mol
1a	CH_3	$ZrClCp_2$	94 (90.4)[c]	120 (120)[c]	137.4	93.6	-9.7
1c	H	$ZrClCp_2$	104.1	120	173.9	66.1	-0.9
2a	$SiMe_3$	Ph	83.3 (89.9)[c]	110 (119)[c]	120.9	108.1	-5.2
3c	CH_3	CH_3	101.6	120	140.8	99.2	-1.0
3f	H	H	120	120	154.8	85.2	+0.2
4[b]	H	$SiMe_3$	127.9	110	150.1 (144.2)[c]	79.9 (-)	+1.9

[a] The values are derived with the extended Hückel procedure. [b] The calculations were carried out with a C–C distance of 1.317 Å. [c] Experimental values in parentheses.

Chart II

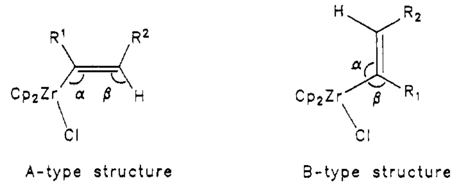

suspected for other such Cp_2Zr—CH═CH—R-containing zirconocene complexes from their NMR data.[8,9]

It has to be noted, however, that some of the structural features of the σ-CH═CHSiMe$_3$ ligand are quite unusual. The C1–C2 bond length is extremely short for a C(sp^2)–C(sp^2) multiple bond. At 1.217 (9) Å it is approaching a value not far from that of a C≡C triple bond (ca. 1.18 Å in organic alkynes;[10] 1.206 (3) Å was the observed C≡C distance in $Cp_2Zr(—C≡CH_3)_2$,[16a] and a typical C═C bond length in a trans-disubstituted olefin is 1.31 Å[10]). The C2–Si separation is quite normal (1.848 (7) Å). However, it is noteworthy that the angles Zr–C1–C2 = 144.2 (5)° and C1–C2–Si = 136.8 (6)° both differ very much from 120°. This may indicate an unusual distortion of the [Zr]—C-H═CH—[Si] double bond in **4** toward a C(sp)–C(sp) multiple bond.[16b] Unfortunately, the hydrogen atoms at carbon centers C1 and C2 were not located. Therefore, it remains unclear whether three-center–two-electron interactions between the metal center and the C^α–H and/or C^β–H σ-bond might be causing this unusual distortion of the metal-bound alkenyl ligand, which is quite different from the secondary interactions observed in the related complexes **5** and **6**.

Model Calculations. To elucidate the geometry, the electronic structure, and possible agostic interactions, we have carried out model calculations using the extended Hückel method. In these investigations we focused on three questions: (i) Is the deviation of the Zr–C1–C2 angle α from 120° (see Table V) mainly due to steric and/or electronic effects? (ii) Does the reduction of α lead to an agostic interaction between the metal and the β-C-H bond (type A) or the α-C-H bond (type B)? (iii) What is the influence of R_1 and R_2 (see Table V) on the structure of type A and type B complexes?

To study possible agostic interactions of A-type complexes, we varied the angles α and β. For a similar study on B-type complexes only α was varied. The model compounds we chose are listed in Table V. The geometrical parameters we set out with in the case of **1a**, **2a**, and **4** were those reported from single-crystal X-ray investigations on these compounds. For model compounds **1c** and **3f** we used standard parameters. In the calculations on **2a** and **4** the SiMe$_3$ group was replaced by the SiH$_3$ moiety.

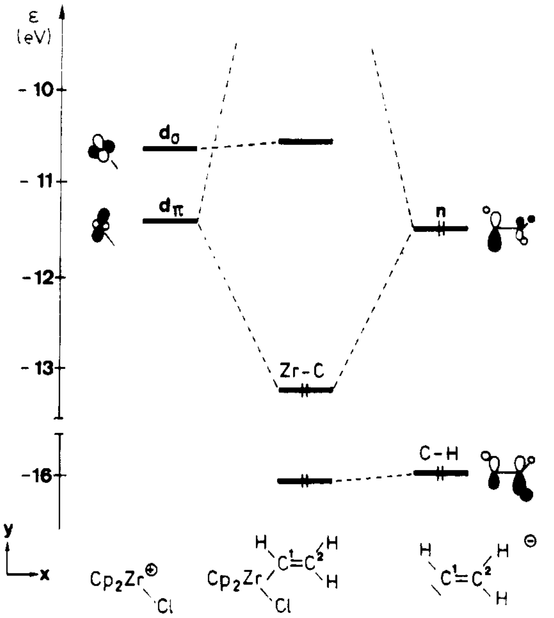

Figure 3. Diagram of the interaction between the frontier orbitals of a Cp_2ZrCl^+ fragment and $C_2H_3^-$ to yield $Cp_2ZrCl(C_2H_3)$. The orbital energies are derived from an extended Hückel calculation.

The potential energy surface shows one global minimum for the α and β values given in Table V; no local minima are present. We notice a fairly good agreement between the calculated and measured values for α and β in those cases (**1a**, **2a**) where X-ray data are available. Agostic interactions (α < 120°) are predicted for those A-type examples where R_1 and R_2 are large groups. A comparison between the predicted energies for type A and type B complexes shows only small differences. This is anticipated because both types represent rotamers. A free rotation around the Zr–C bond is, however, hindered by the Cp substituents.

It is found that for **1a**, **1c**, **2a**, and **3c** the A type should be more stable than the B conformer. For **3f** and **4** the B-type arrangement should be preferred. The calculations predict for **3f** and **4** in the B-type conformation a close proximity between the C1–H bond and the metal. In those cases where R_1 represents a large group (e.g. SiMe$_3$), the type A structure seems to be preferred due to a repulsion that takes place in the B conformer between Cl and the substituent. For CpZrCl(PhC═CMe$_2$), however, the B-type conformation has been reported,[15] but in this case the conformation is such that the plane of the phenyl ring is orthogonal to the alkenyl–chlorine plane and therefore steric repulsion is a minimum for the type B conformation. The strong dependence of α on the size of R_1 suggests that steric effects play a major role. As we will see in the next

---

(16) (a) Erker, G.; Frömberg, W.; Benn, R.; Mynott, R.; Angermund, K.; Krüger, C. *Organometallics* **1989**, *8*, 911. (b) A subsequent high-resolution structural investigation of **4** based on 45 059 reflections at 100 K reveals a disorder problem as the source of the artificial distortion of the —CH═CH—Si group. Correct values are C1═C2 1.343 (2) Å, C1—C2—Si 127.5 (1)°, Zr—C1—C2 136.0 (1)° (Krüger, C.; Erker, G. To be submitted for publication).

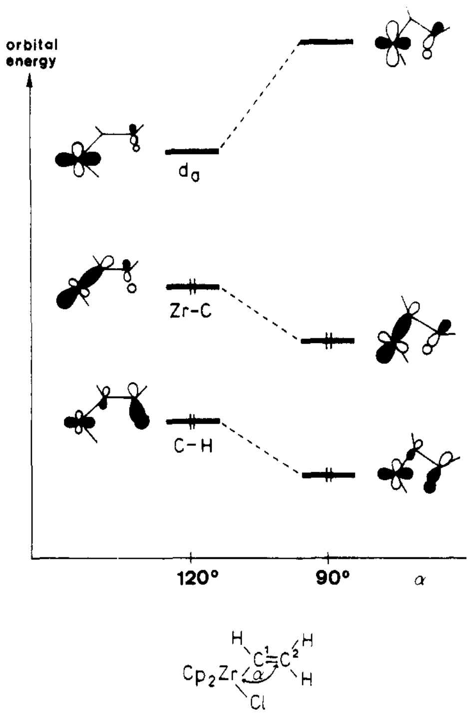

Figure 4. Qualitative correlation diagram between the valence orbitals of $Cp_2ZrCl(C_2H_3)$ of type A conformation for $\alpha = 120$ and 90°.

section, electronic effects are also important.

MO Analysis. (1) Type A Structures. The electronic structure of the alkenylzirconocene complexes can be derived by applying Hoffmann's fragment MO approach.[17] The valence orbitals of **2a** can be constructed from those of a Cp_2ZrCl^+ fragment and of a $CH{=}CH_2^-$ moiety. The four highest occupied MO's of the metallocene moiety are mainly localized at the ligands and can be described as π MO's of the Cp rings.[17] Important for our discussion are two low-lying empty MO's which are strongly localized at the metal center (see left side of Figure 3). Both fragment MO's result from the $1a_1$, b_2, and $2a_1$ set of a bent zirconocene,[12] by adding a chlorine atom to it in a nonlinear fashion. This will give rise to a Zr–Cl σ-bond and two empty low-lying MO's that can be described as linear combinations of the $4d_{z^2}$, $4d_{x^2-y^2}$, and $4d_{xy}$ atomic orbitals of zirconium. While the one designated d_σ MO points mainly in the x direction, the d_π MO is directed toward the diagonal of the x,y plane. Further unoccupied MO's of the Cp_2ZrCl fragment are predicted at rather high energy compared to d_π and d_σ and are not significant for our further discussion; therefore, they are omitted in Figure 3. For the olefinic ligand our calculations predict four high-lying occupied MO's. Two of them, which can be described as the C–C σ bond and the C–C π bond, are omitted for the sake of clarity. The two remaining ones can be described as the lone pair at the carbon (n) and the C–H σ bond (see right side of Figure 3). For reasons of symmetry both mix with each other. As anticipated, the addition of the vinylic anion along the x,y diagonal leads mainly to an interaction between the lone pair n and d_π while the others remain essentially unchanged. As a result a low-lying empty MO (d_σ) remains as it should be in a 16-electron species.

The resulting species ($\alpha = 120°$) can further be stabilized by allowing the interaction between the empty d_σ MO and the C–H σ-bond. This is demonstrated in the Walsh-type diagram in Figure 4. On the left side of Figure 4 we show a schematic drawing of the wave functions of the two occupied MO's d_π + n (which can be described as the Zr–C σ-bond in a localized picture) and the C–H σ-bond for $\alpha = 120°$, together with the LUMO. For the occupied MO's we notice an in-phase relation between the C–H σ-bond and the metal orbital; for the LUMO this relation is an out-of-phase one. The reduction of α, which brings the C2–H bond and the metal center closer together, leads to a stabilization of the two occupied MO's and to a destabilization of the LUMO.

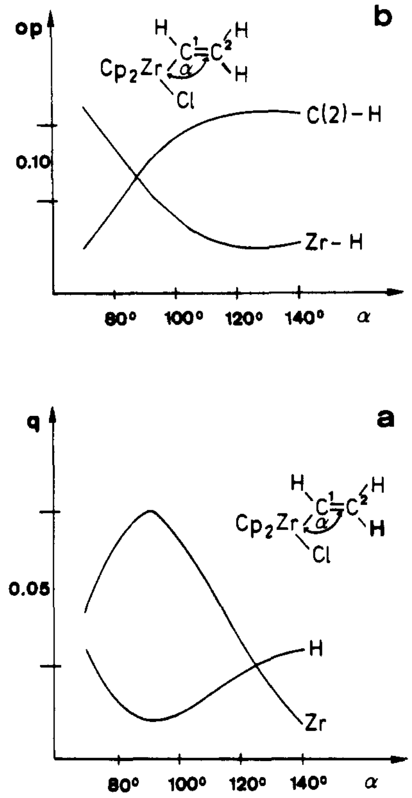

Figure 5. (a) Change of the electron density, q, on the Zr and H atoms at C2 of $Cp_2ZrCl(C_2H_3)$ as a function of α. (b) Change of the reduced overlap population (op) of the Zr–H and C2–H bonds of $Cp_2ZrCl(C_2H_3)$ as a function of α.

As a result of these changes a charge transfer from the C2–H σ-bond to the metal occurs. This is demonstrated in Figure 5a, where the calculated net charge at C2 and Zr is shown as a function of α. In Figure 5b the reduced overlap populations for the C–H bond at C2 and the Zr–H bond are shown as a function of α. This figure makes clear how sizable changes in the bond strengths are observed below $\alpha = 110°$ when the steric requirements for agostic interactions are met. The overlap population of the C2–H bond decreases substantially due to transfer of electron density from this C–H bond to Zr from an angle of 110° downwards. It is interesting to note that at the same time the overlap population of the Zr–H bond increases (Figure 5b).

(2) Type B Structures. As a model for probing B-type structures we also chose **3f** ($Cp_2ZrCl(CH{=}CH_2)$). The interaction diagram between the Cp_2ZrCl^+ moiety and the $CH{=}CH_2^-$ fragment looks very similar to that shown in Figure 3. For geometrical reasons the interaction between the C2–H bond and the metal is less likely than in A-type structures. Once the values of α are larger than 120°, agostic interactions between the metal and the C1–H bond are possible. The Walsh-type diagram in Figure 6 sum-

---

[17] Albright, T. A.; Burdett, J. K.; Whangbo, M. H. *Orbital Interactions in Chemistry*; Wiley: New York, 1985.

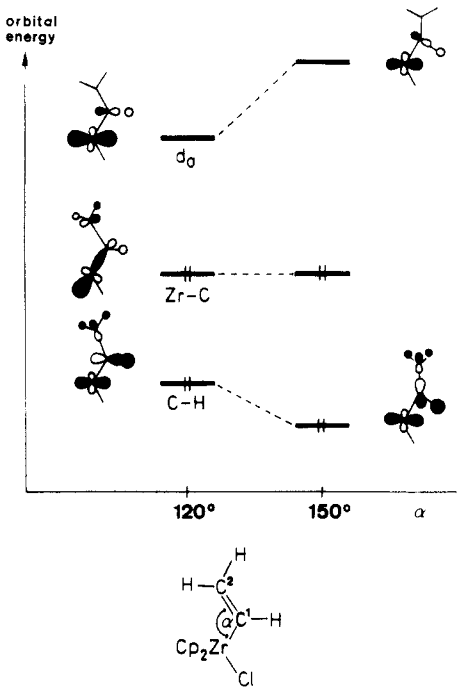

Figure 6. Qualitative correlation diagram between the valence orbitals of $Cp_2ZrCl(C_2H_3)$ of type B conformation for α = 120 and 150°.

marizes the agostic interactions that occur for B-type structures. In contrast to the A type only the C–H σ-bond is stabilized while the Zr–C σ-bond is not affected. Similar to the results shown in Figure 5 we obtain for A-type structures a reduction of the overlap population of the C1–H bond with increasing α from 120 to 150°. This is also due to a charge transfer from the C–H bond to the metal. At the same time the overlap population for the Zr–H bond increases.

Discussion

The alkenylzirconocene halides **2a,b** are remarkable molecules in two ways. Eisch et al. have recently inserted phenyl(trimethylsilyl)acetylene into the metal–carbon σ-bond of cationic Cp_2TiCH_3 to give **5**.[14a] The same regioselectivity was observed as for the hydrozirconation reaction of $Me_3SiC{\equiv}CPh$ reported here yielding **2**; i.e., the bulky trimethylsilyl group ends up in the α-position at the σ-alkenyl ligand adjacent to the transition-metal center. However, the $[M]C(SiMe_3){=}CRPh$ complexes **2** (M = Cp_2ZrX, R = H) and **5** (M = Cp_2Ti^+, R = CH_3) are structurally very different. There is evidence that **5** contains an agostic Ti–C–Si interaction. Evidence for this comes from model calculations by Morokuma et al.[14b] The observed very small Ti–C1–Si angle (89°) of **5** is in accord with this interpretation. The less electrophilic neutral Cp_2ZrX center in **2** clearly does not support the analogous agostic Zr–C–Si interaction (the Zr–C1–Si angle is 139.3 (1)° for **2a** and 139.4 (3)° for **2b**). We thus conclude that formation of a β-CH agostic interaction is superior to metal coordination of an adjacent Si–C bond in the given competitive situation.

The inductive effect of a Si center could lead to an increase of the donor properties of an adjacent C–H bond and thereby support the tendency of forming the M–H–C agostic bond. However, there is no evidence for such an electronic effect being of major importance for the formation of the β-CH agostic complexes **2**. The Me_3 Si group here ends up in the "wrong" position for electronically supporting the Zr–H–C bond formation. It is the C–H bond adjacent to the (inductively) electron-withdrawing phenyl substituent that coordinates to the weakly Lewis acidic zirconium center of the bent metallocene unit. Moreover, the Me_3Si substituent of $Cp_2ZrCl(-CH{=}CHSiMe_3)$ (**4**) is in the right place to electronically support the β-CH agostic bond formation. Such an interaction is, however, absent in the alkenylmetallocene complex **4**.

It appears that the formation of the agostic β-C–H–M interaction in the complexes **2**, exhibiting only a weakly electrophilic transition-metal center, is dominated by steric effects. Steric pressure between bulky alkenyl substituents, cis-orientated at C1 and C2, in addition to an unfavorable steric interaction between the large metal complex fragments at C1 (Cp_2ZrX and Me_3Si), causes sufficient deformation of the σ-framework as to bring the alkenyl β-CH bond into the vicinity of the 16-electron transition-metal center. Varying the Zr–C1–Si and Zr–C1–C2 angles in our model calculations supports this view. The β-CH bond, once brought into the vicinity of the Zr center, is coordinated to form a stable three-center–two-electron interaction.

While electronic effects have been discussed on several occasions for agostic early-[18] and late-transition-metal[19] complexes, the role of steric factors has largely been neglected. Our experimental work and the model calculations presented here demonstrate that for the vinylic zirconocene complexes in question steric *and* electronic factors are important for building an agostic M–H–C interaction.

Experimental Section

Organometallic compounds were handled under an argon atmosphere with use of Schlenk-type glassware. Solvents were distilled under argon from potassium/benzophenone, lithium aluminum hydride, sodium potassium alloy, or P_4O_{10} (Sicapent, Merck) prior to use. The hydrozirconation reagent ($Cp_2Zr(H)Cl$) was prepared from Cp_2ZrCl_2 and $LiAlH_4$ in tetrahydrofuran. Substituted acetylenes were prepared according to literature procedures. NMR spectra were obtained with a Bruker WP 200 SY NMR spectrometer. Melting points were measured with a Büchi SMP-20 apparatus and are not corrected. Elemental analyses were performed by Dornis and Kolbe, Mikroanalytisches Laboratorium, Mülheim a. d. Ruhr, FRG, and the Institut für Anorganische Chemie der Universität Würzburg.

(*E*)-1-[Bis(cyclopentadienyl)chlorozirconio]-1-(trimethylsilyl)-2-phenylethene (2a). A suspension of 2.29 g (8.88 mmol) of hydridozirconocene chloride in 25 mL of toluene is stirred for 17 h with 1.74 g (9.98 mmol) of phenyl(trimethylsilyl)acetylene at 18 °C. The resulting red solution is concentrated in vacuo to a volume of 5 mL. Pentane (40 mL) is added. The resulting precipitate is recovered by filtration, washed twice with 5-mL portions of pentane, and dried in vacuo (3.09 g crude product, 79%). The purification of this material can be carried out in two ways. Successive washings with pentane (15 × 10 mL) gave analytically pure **2a** (39%). Alternatively, crystallization of the crude material from 10 mL of toluene at –20 °C yielded pure crystalline **2a** in 33% yield; mp 136 °C dec. Anal. Calcd for $C_{21}H_{25}SiClZr$ (M_r = 432.19): C, 58.36; H, 5.83. Found: C, 58.36; H, 6.20. ^1H NMR (benzene-d_6): δ 0.17 (s, 9 H, $SiMe_3$), 5.80 (s, 10 H, Cp), 6.95–7.16, 7.40–7.47 (m, 5 H, Ph), 8.59 (s, 1 H, CH). ^{13}C NMR ($CDCl_3$): δ 1.6 ($SiMe_3$), 111.6 (Cp), 113.3 ($^1J_{CH}$ = 123 Hz, $=C^{\beta}H-$), 206.8 ($-C^{\alpha}=$), 127.5, 128.2, 129.0, 136.0 (Ph).

(*E*)-1-[Bis(cyclopentadienyl)bromozirconio]-1-(trimethylsilyl)-2-phenylethene (2b). Lithium bromide (3.30 g, 38.02 mmol) is stirred for 5 h with a solution of 3.10 g (7.18 mmol) of **2a** in 200 mL of ether at 18 °C. Ether is then removed in vacuo. The residue is taken up with 20 mL of toluene and the solution

---

[18] Koga, N.; Obara, S.; Morokuma, K. *J. Am. Chem. Soc.* **1984**, *106*, 4625. Demolliens, A.; Jean, Y.; Eisenstein, O. *Organometallics* **1986**, *5*, 1457.

[19] Fitzpatrick, N. J.; McGinn, M. A. *J. Chem. Soc., Dalton Trans.* **1985**, 1637. Koga, N.; Obara, S.; Kitaura, K.; Morokuma, K. *J. Am. Chem. Soc.* **1985**, *107*, 7109.

filtered. The filtrate is concentrated in vacuo to a volume of 5 mL. Hexane (20 mL) is added with rapid stirring. The slightly yellow precipitate is recovered by filtration, washed once with 2 mL of hexane, and dried in vacuo to give 2.35 g (69%) of **2b**, mp 136–137 °C dec. Anal. Calcd for $C_{21}H_{25}SiBrZr$ (M_r = 476.64): C, 52.92; H, 5.29. Found: C, 52.93; H, 5.24. MS (70 eV): *m/e* 480–474 [M^+; observed (calculated) relative intensities 0.28 (0.30), 0.10 (0.15), 0.53 (0.57), 0.38 (0.43), 1.00 (1.00), 0.34 (0.35), 0.70 (0.69)]. ^1H NMR (benzene-d_6): δ 0.20 (s, 9 H, $SiMe_3$), 5.77 (s, 10 H, Cp), 7.00–7.12, 7.52–7.61 (m, 5 H, Ph), 8.41 (s, 1 H, CH). ^{13}C NMR (methylene-d_2 chloride): δ 1.5 ($^1J_{CH}$ = 121 Hz, $SiMe_3$), 109.4 ($^1J_{CH}$ = 120 Hz, $=C^{\beta}H$), 204.5 ($-C^{\alpha}=$), 111.7 (Cp), 128.1, 128.7, 129.7, 135.5 (Ph).

(*E*)-1-[Bis(cyclopentadienyl)iodozirconio]-1-(trimethylsilyl)-2-phenylethene (2c). Likewise, 650 mg (1.50 mmol) of **2a** and 460 mg (3.43 mmol) of lithium iodide were stirred together in 50 mL of ether for 5 h at 18 °C. Similar workup with dissolution in 10 mL of toluene, filtration and concentration to 2 mL, and precipitation with 10 mL of hexane gave 530 mg (67%) of **2c**, mp 151–152 °C dec. Anal. Calcd for $C_{21}H_{25}SiIZr$ (M_r = 523.65): C, 48.17; H, 4.81. Found: C, 47.61; H, 5.08. ^1H NMR (benzene-d_6): δ 0.22 (s, 9 H, $SiMe_3$), 5.72 (s, 10 H, Cp), 7.00–7.10, 7.65–7.72 (m, 5 H, Ph), 7.85 (s, 1 H, CH). ^{13}C NMR (methylene-d_2 chloride): δ 1.3 ($^1J_{CH}$ = 118 Hz, $SiMe_3$), 104.1 ($^1J_{CH}$ = 111 Hz, $=C^{\beta}H$), 198.7 ($-C^{\alpha}=$), 111.0 (Cp), 128.3, 128.7, 129.8, 133.7 (Ph).

(*E*)-1-[Bis(cyclopentadienyl)chlorozirconio]-2-(trimethylsilyl)ethene (4). A mixture of 3.10 g (12.02 mmol) of hydridozirconocene chloride and 1.18 g (12.01 mmol) of (trimethylsilyl)acetylene is stirred in 50 mL of toluene for 4 h at 18 °C. The dark red solution is filtered. The filtrate is concentrated in vacuo to a volume of 5 mL. Pentane (30 mL) is added to precipitate the product. Filtering followed by washing with pentane (5 × 5 mL) and drying in vacuo yields 1.90 g (44%) of **4**, mp 99–101 °C dec. Anal. Calcd for $C_{15}H_{21}SiClZr$ (M_r = 356.10): C, 50.59; H, 5.94. Found: C, 50.39; H, 5.72. ^1H NMR (benzene-d_6): δ 0.15 (s, 9 H, $SiMe_3$), 5.82 (s, 10 H, Cp), 6.63, 8.03 (AB, ^3J = 22.5 Hz, Si—CH=CH—Zr). ^{13}C NMR (benzene-d_6): δ −0.9 ($^1J_{CH}$ = 119 Hz, $SiMe_3$), 112.9 (Cp), 143.3 ($^1J_{CH}$ = 136 Hz, =CHSi), 202.7 ($^1J_{CH}$ = 128 Hz, ZrCH=).

X-ray Crystal Structure Determinations: **2b**, $C_{21}H_{25}BrSiZr$, M_r = 476.6, monoclinic, $P2_1/n$, a = 9.746 (1) Å, b = 17.968 (3) Å, c = 11.887 (1) Å, β = 90.46 (1)°, V = 2081.6 Å^3, Z = 4, d_{calc} = 1.52 g cm^{-3}, μ = 24.77 cm^{-1}, Enraf-Nonius CAD 4 diffractometer, 4853 measured reflections, 2937 observed reflections ($I > 2\sigma(I)$), R = 0.051 and R_w = 0.049 ($w = 1/\sigma^2(F_o)$) for 221 parameters; **4**, $C_{15}H_{21}ClSiZr$, M_r = 356.1, monoclinic, $P2_1/c$, a = 10.866 (1) Å, b = 12.457 (1) Å, c = 13.373 (2) Å, β = 110.80 (1)°, V = 1692.1 Å^3, Z = 4, d_{calc} = 1.40 g cm^{-3}, μ = 8.51 cm^{-1}, Enraf-Nonius CAD 4 diffractometer, 4149 measured reflections, 2623 observed reflections ($I \geq 2\sigma(I)$), R = 0.046 and R_w = 0.048 ($w = 1/\sigma^2(F_o)$) for 163 parameters. Further details concerning the X-ray data collections and the structure determinations are given in the supplementary material.

Acknowledgment. Generous financial support from the Stiftung Volkswagenwerk (grant to R.G. and G.E.), the Fonds der Chemischen Industrie, the Bundesminister für Forschung und Technologie (C.K. and G.E.), and the Alfried Krupp von Bohlen und Halbach-Stiftung (G.E.) is gratefully acknowledged.

Registry No. **1a**, 105036-31-5; **1c**, 124380-44-5; **2a**, 119747-83-0; **2b**, 124380-42-3; **2c**, 124380-43-4; **3c**, 124380-45-6; **3f**, 81894-89-5; **4**, 124380-41-2; $Cp_2Zr(H)Cl$, 37342-97-5; $Me_3SiC{\equiv}CPh$, 2170-06-1; $HC{\equiv}CSiMe_3$, 1066-54-2.

Supplementary Material Available: Details of the X-ray data collection and structure determination of **2b** and **4** and lists of bond lengths and angles, atomic fractional coordinates, and thermal parameters (16 pages); listings of observed and calculated structure factors of **2b** and **4** (27 pages). Ordering information is given on any current masthead page.